VNU Journal of Science: Mathematics - Physics

Journal homepage: https://js.vnu.edu.vn/MaP

Original Article

The Structural Characteristics and Phase Transformation in Al_2O_3 Glass. A Molecular Dynamics Simulation

Tran Thi Quynh Nhu[1,5], Pham Huu Kien[1,*], Phan Dinh Quang[1], Nguyen Hai Yen[1,3], Vu Thi Thanh Huong[3], Dao Ngoc Dung[4], Giap Thi Thuy Trang[1]

[1]*Thai Nguyen University of Education, 28 Luong Ngoc Quyen, Thai Nguyen, Vietnam*

[2]*Hanoi University of Technology, 1 Dai Co Viet, Hanoi, Vietnam*

[3]*Vietnam Northern Upland High School, Z 115 Quyet Thang, Thai Nguyen, Vietnam*

[4]*Hoa Thuong Junior High School, Dong Hi, Thai Nguyen, Vietnam*

[5]*Tuyen Quang High School for Gifted Students, Tran Hung Dao, Tuyen Quang, Vietnam*

Received 17 July 2021
Revised 16 August 2021; Accepted 16 August 2021

Abstract: In this work, we have performed a simulation to study the structural characteristics and phase transformation in Al_2O_3 glass under compression. The structural characteristics of Al_2O_3 glass were examined via AlO_x units, OAl_y linkages, the average bond distance distributions, order parameters, and visualization of simulation data. The result showed that the network structure of Al_2O_3 glass is built mainly by AlO_x (x = 3, 4, 5, 6, 7) units that are linked to each other via common O atoms. We found that the distribution of AlO_x units in network structure is not uniform but tends to form clusters contained AlO_x units. In addition, during a moderately long time, the glass has a two-phase that consists of separate low-density (LD) and high-density (HD) phases. The size of these phases significantly depends on the compression.

Keywords: Simulation, structure, cluster, phase, low-density, high-density.

1. Introduction

Alumina(Al_2O_3) is a very important ceramic material used in many applications. It is known that Al_2O_3 glass is a network-forming, whose structure consists of a three-dimensional network of oxygen-

* Corresponding author.
E-mail address: phkien80@gmail.com

https//doi.org/10.25073/2588-1124/vnumap.4663

shared AlO_4 tetrahedrons. At ambient pressure, the Al-O bond length is close to 1.72 ± 0.02 Å. The average tetrahedral angle shows a maximum at 141° ± 5°. In addition, the strong directional bonds and high degree of intermediate range order are found to persist in the glass phase [1-9]. Many experimental studies of Al_2O_3 glass [2-6] confirmed that Al-O coordination number increases from four-fold to six-fold between 10 and 25 GPa, resulting in a network of SiO_6 octahedrons.

Simulation techniques also provide details about the microstructural properties, as well as the glass-glass phase transformation at atomic levels. The molecular dynamics (MD) simulation with applied effective potentials [7-10] reproduces well the structural factors obtained experimentally, but the bond angle distribution is rather broad to be compatible with experimental data. Although *ab*-initio simulation confirmed that the presence of strong directional bonds and gives better agreement with experimental data [11, 12], its application is limited due to very small models realized. The previous simulations provided evidence of the glass-glass phase transformation; many aspects of this phenomenon remain unclear. Therefore, in this work, we focus on studying the structural characteristics and indicating the existence of two phases with high- and low-density of Al_2O_3 glass. The properties of Al_2O_3 can be inferred from simulated models by the bond length, bond-angle, coordination number, and cluster function [13, 14].

2. Computational Procedure

MD simulation has been done in the cubic box with periodic boundary condition for 2,000 atoms (800 Al and 1,200 O atoms). We use the Born-Mayer type pair potential to construct the Al_2O_3 glass models. The form of the potential is

$$U_{ij}(r_{ij}) = Z_i Z_j \frac{q_i q_j}{r_{ij}} + B_{ij} \exp\left(-\frac{r_{ij}}{R_{ij}}\right) \quad (1)$$

The terms in eq. (1) represent Coulomb and repulsion energy, respectively. Here r_{ij} is the interatomic distance between atom i and j; q_i and q_j are the charges of i^{th} and j^{th} ions; B_{ij} and R_{ij} are parameters accounting the repulsion of the ions shells as listed in Table 1. The long-range Coulomb interactions are calculated with the standard Ewald simulation method. The equations of motion are integrated with Verlet algorithm, here we use a time step of 0.4 fs.

Table 1. The potential parameters for Al_2O_3 glass, as seen in ref. [9-11]

Pairs	B_{ij} (eV)	R_{ij} (Å^{-1})	q_i, q_j (eC)
Al-Al	0.0	0.0	q_{Al} = +3.0
Al-O	1479.86	3.4483	q_O = -2.0
O-O	1500	3.4483	-

This initial configuration is heated to 6,000 K at zero pressure and relaxed over 5×10^4 time steps. Then, the model is cooled to 3,000; 1,000 and finally to 300 K, at zero pressure during 3×10^4 time steps. Next, the system is allowed to reach equilibrium for over 10^5 time steps. With this well-equilibrated model, we prepared 6 models with pressure of 5, 10, 15, 20, 25, 30 GPa, temperature of 300 K. After that the models has been relaxed in NVE ensemble (the constant volume and energy) for 5×10^4 time steps, to reach the equilibrium. The network structure is studied via AlO_x and OAl_y basic units. The cutoff distance r_{cutoff} used equals 2.4 Å which is chosen from first minimum of the pair radial distribution function $g_{Al\text{-}O}(r)$.

3. Results and Discussion

The radial distribution function (RDF) $G_N(r)$ allows to determine the average number of atoms at any given atomic distance. Figure 1 displays the total RDFs $G_N(r)$ of Al_2O_3 glass at different pressures, temperature of 300 K and experimental data reported by Lamparter (1997) [4].

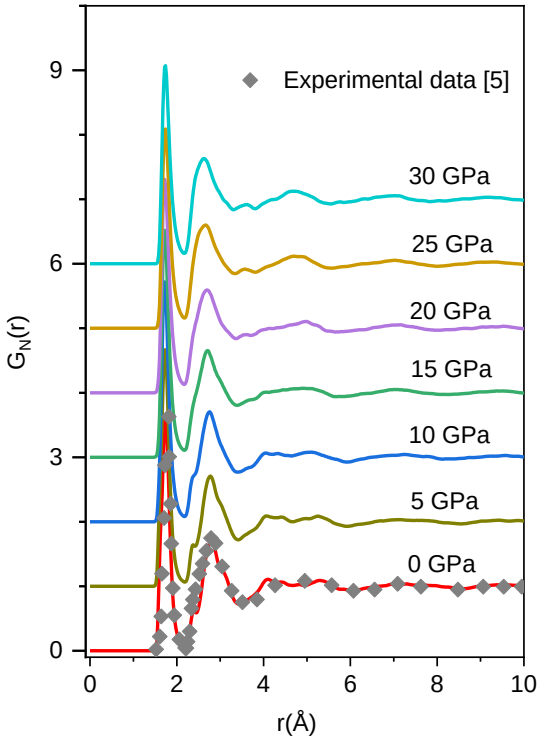

Figure 1. The total RDFs $G_N(r)$ of Al_2O_3 model at different pressures and temperature of 300 K and experimental data reported by Lamparter (1997).

The total RDF $G_N(r)$ is calculated from pair RDFs $G_{Al\text{-}O}(r)$, $G_{Al\text{-}Al}(r)$, $G_{O\text{-}O}(r)$, it is defined by

$$G_N(r) = \frac{\sum_{\alpha\beta} C_\alpha f_\alpha C_\beta f_\beta G_{\alpha\beta}(r)}{\left[\sum_\alpha C_\alpha f_\alpha\right]^2} \quad (2)$$

Here, C_α, C_β are the number fraction of species α, β; f_α, f_β are the corresponding coherent neutron scattering length of Al and O atoms; $G_{\alpha\beta}(r)$ is pair RDFs $G_{Al\text{-}O}(r)$, $G_{Al\text{-}Al}(r)$, $G_{O\text{-}O}(r)$.

We take $f_{Al}=0.34493\times10^{-14}$m, $f_O= 0.58053\times10^{-14}$m as used in ref. [5, 13]. Figure 1 shows that the calculated $G_N(r)$ (at ambient pressure) is in good agreement with the experimental data [4]. It is known that the total RDFs exhibit the short-range order (SRO). As seen, with increasing pressure, the first peak shifts to the right from 1.74 ± 0.01 to 1.72 ± 0.01 Å, whereas the second peak shifts to the left from 2.74 ± 0.01 to 2.58 ± 0.01 Å. The shift of these peaks has also been confirmed by other works [1-5]. Note that the first peak of $G_N(r)$ is contributed from the pair $G_{Al\text{-}O}(r)$ exhibiting the Al-O bond distance, while the second peak is contributed from the pair $G_{Al\text{-}Al}(r)$, $G_{O\text{-}O}(r)$ exhibiting the Al-Al, O-O bond distance,

respectively. Figure 2 displays an arrangement of Al_2O_3 model at ambient pressure, temperature of 300 K. Here, one can see the AlO_3, AlO_4, AlO_5, AlO_6 units, as well as the OAl_2, OAl_3 and OAl_4 linkages. As seen, AlO_x units connect together via common O atoms to form AlO_x and OAl_y (x = 3-6, y = 2-4) clusters.

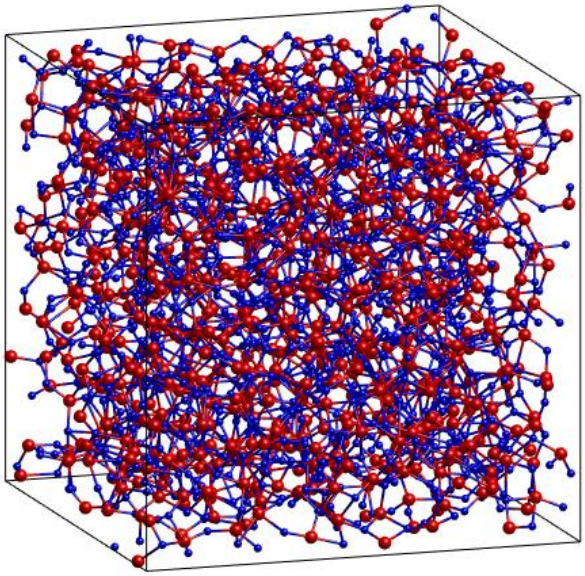

Figure 2. Snapshots of the atomic arrangement of Al_2O_3 model at 0 GPa, and temperature of 300 K. Here Al and O atoms are in red and blue color, respectively.

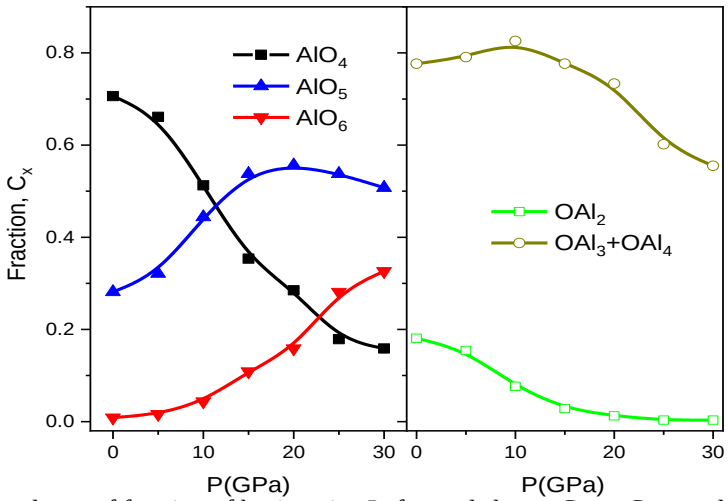

Figure 3. Pressure dependence of fraction of basic units. Left panel shows C_{AlO4}, C_{AlO5} and C_{AlO6} fractions. In the right panel C_{OAl2} and $C_{OAl3+OAl4}$ fractions are shown.

In order to clarify the phase transition phenomena, characteristic of basic units and linkages are considered. Figure 3 shows the fraction of basic units and linkages. Here the fraction of basic units is given as $C_{AlOx} = n_{AlOx}/n_{Al}$; $C_{OAly} = n_{OAly}/n_O$, where n_{AlOx}, n_{OAly}, n_{Al}, n_O is the number of AlO_x, OAl_y, Al and O, respectively. As seen, C_{AlO4} monotonously decreases with increasing pressure, while

C_{AlO6} increases, C_{AlO5} reaches maximum about 22 GPa, and then decreases with increasing pressure. This demonstrates that there is a transformation from tetrahedral to octahedral structure. Moreover, fraction C_{OAl2} monotonously decreases with increasing pressure, while the fraction C_{OAl2} reaches maximum at 12 GPa, and then decreases. This indicates that in the high-pressure range, the AlO_5, AlO_6 units linked each other via three common O atoms significantly increases, indicating the density of Al_2O_3 glass in the high-pressure range is larger than the one in high-pressure range. We note that the curve for C_{AlO5} intersects with the one for C_{AlO4} and C_{AlO5} at 12 ± 0.5 and 22 ± 0.5 GPa, respectively. It means that the transformation from tetrahedral to octahedral structure mainly occurs in the pressure range of 12-22 GPa.

Next, in order to get some insights into the glass-glass transition in Al_2O_3 glass, we have used the order parameter, it is defined by

$$\eta(P) = \frac{n_6 - n_4}{n_6 + n_4} \tag{3}$$

Here, n_4 and n_6 are the numbers of four-fold and six-fold coordinated Al atoms to oxygen. Note that if $\eta(P) = -1$ there is no six-fold coordination in the system and analogously if $\eta(P) = 1$ there is no four-fold coordination. The order parameter is plotted in Figure 4 as a function of pressure, and no abrupt change from a tetrahedral to an octahedral order has been found due to the existence of the five-fold coordinated unit AlO_5 in the system. This means that the first-order nature of the glass-glass transition in Al_2O_3 glass is not found clearly. They gradually change in Al_2O_3 glass.

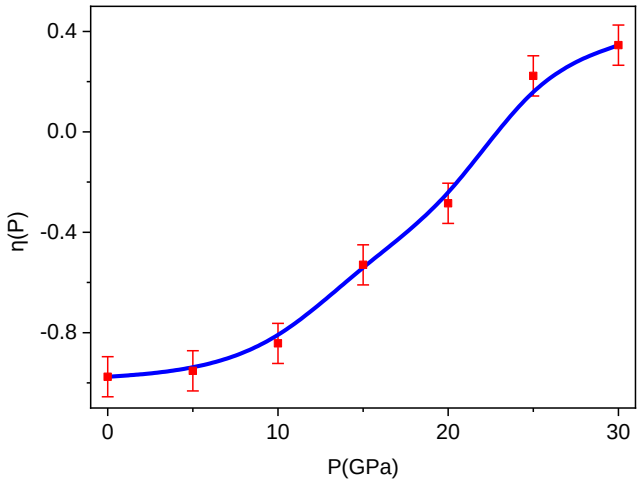

Figure 4. The pressure dependence of the order parameter η of Al_2O_3 model at different pressures.

Under compression, the average Al-O bond length is almost not changed, while that Al-Al, O-O bond length tends to decrease, i.e, from 3.14 Å (at ambient pressure) to 2.98 Å (at 30 GPa) for Al-Al pair, and from 2.80 to 2.58 Å for O-O pair. This demonstrates that the structure of Al_2O_3 glass has a tendency to become more packing under compression. In other words, there is the transformation from LD-phase to HD-phase with increasing pressure. This result is also showed as confirmed from Figure 4 and 5.

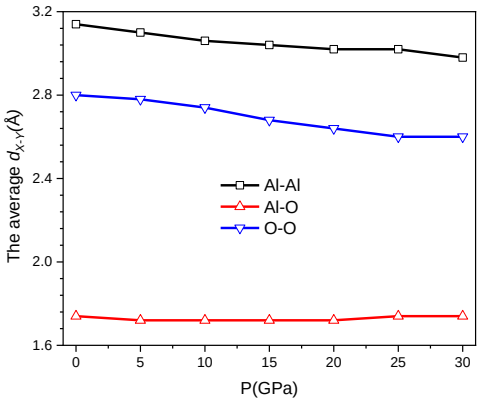

Figure 5. Evolution of the average d_{Al-Al}, d_{Al-O} and d_{O-O} bond distances as a function of pressure for glass Al_2O_3 model.

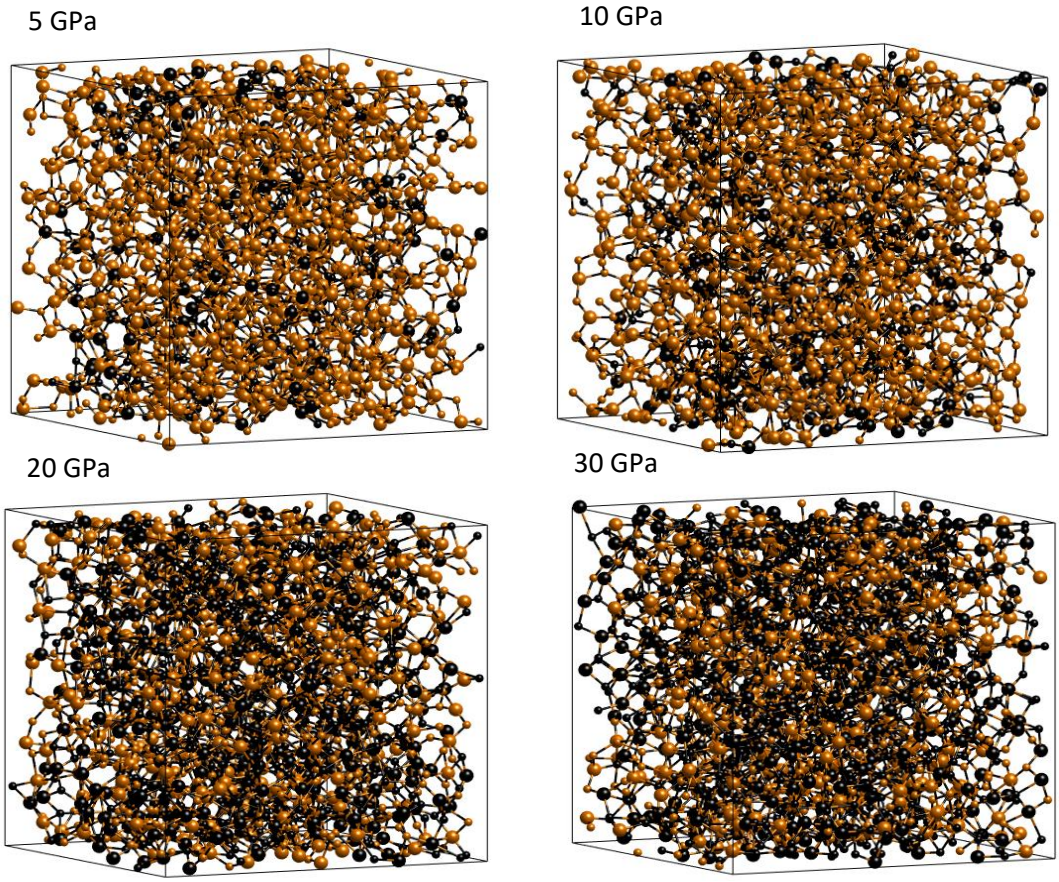

Figure 6. Snapshot of the positions of atoms in LD-phase (AlO_4 units) and HD-phase (AlO_5, AlO_6 units of Al_2O_3 model at 5, 10, 20 and 30 GPa. Here, the yellow, black spheres represent the atoms in LD-phase and HD-phase, respectively.

The above analysis indicates that at the lower pressure 12 GPa, LD-phase is dominant, conversely, beyond 22 GPa, HD phase is dominant. In the range of 12-20 GPa, Al_2O_3 glass is the mixing of two phases (intermediate phases). In order to clarify the polyamorphism and the phase transformation in the Al_2O_3 glass, the network structure has been visualized at the atomic level. Figure 6 shows the distribution of AlO_x in models. As seen, the distribution of AlO_x units is not uniform but it tends to cluster forming regions of LD. Conversely, the AlO_5 and AlO_6 tend to cluster forming regions of HD. The size of LD and HD regions strongly depends on pressure. Below 12 GPa, the structure of the Al_2O_3 glass is mainly formed from LD phases. As the pressure increases, the size of LD regions decreases while the size of HD regions is increased. In the range of 10-22 Gpa, the structure of the Al_2O_3 glass is mainly formed from two-phases, characteristic of AlO_4, AlO_5 units formed intermediate phases. Beyond 22 GPa, the structure of the Al_2O_3 glass is mainly formed from HD-phases, characteristic of AlO_5, AlO_6 units. Thus, we conclude that at a certain pressure, the structure of Al_2O_3 glass comprises both two phases.

4. Conclusion

We successfully performed a simulation of Al_2O_3 glass with pressure ranging from 0 to 30 GPa, at a temperature of 300 K. The structural characteristics of the constructed models are in good agreement with both the experimental and other simulation data. The result shows that the network structure of Al_2O_3 glass is built mainly by AlO_x (x = 3-7) units that are linked to each other via common O atoms. The distribution of AlO_x units in network structure is not uniform but tends to form clusters which comprise AlO_x units. The cluster of AlO_4 forms a LD-phase, conversely, the cluster of AlO_5 and AlO_6 form HD-phase. During a moderately long time, the Al_2O_3 glass has a two-phase that consists of separate LD- and HD- phases. The size of these phases significantly depends on the compression pressure.

Acknowledgement

The authors are grateful to Prof. P.K. Hung (E-mail: pkhung@fpt.vn) for helpful comments on the manuscript. This research is funded by Science and Technology Research Program at University of Education - Thai Nguyen University for Grassroots Project. Subject code ĐH2022-TN04-02

References

[1] L. Hennet, D. Thiaudiere, M. Gailhanou, C. Landron, J. P. Coutures, D. L. Price, Fast X-ray Scattering Measurements on Molten Alumina Using a 120 Curved Position Sensitive Detector, Review of Scientific Instruments, Vol. 73, No. 1, 2002, pp. 124-129, https://doi.org/10.1063/1.1426228.

[2] Y. Waseda, K. Sugiyama, J. M. Toguri, Direct Determination of the Local Structure in Molten Alumina by High Temperature X-Ray Diffraction, Zeitschrift für Naturforschung A, Vol. 50, No. 8, 1995, pp. 770-774, https://doi.org/10.1515/zna-1995-0809.

[3] S. Ansell, S. Krishnan, J. K. R. Weber, J. J. Felten, P. C. Nordine, M. A. Beno, D. L. Price, M. L. Saboungi, Structure of Liquid Aluminum Oxide, Physical Review Letters, Vol. 78, No. 3, 1997, pp. 464-470, https://doi.org/10.1103/PhysRevLett.78.464.

[4] P. Lamparter, R. Kniep, Structure of Glass Al_2O_3, Physica B: Condensed Matter, Vol. 234, 1997, pp. 405-406, https://doi.org/10.1016/S0921-4526(96)01044-7.

[5] C. Landron, L. Hennet, T. E. Jenkins, G. N. Greaves, J. P. Coutures, A. K. Soper, Liquid Alumina: Detailed Atomic Coordination Determined from Neutron Diffraction Data Using Empirical Potential Structure Refinement, Physical Review Letters, Vol. 86, No. 21, 2001, pp. 4839-4844, https://doi.org/10.1103/PhysRevLett.86.4839.

[6] L. B. Skinner, A. C. Barnes, P. S. Salmon, L. Hennet, H. E. Fischer, C. J. Benmore, S. Kohara et al., Joint Diffraction and Modeling Approach to the Structure of Liquid Alumina, Physical Review B, Vol. 87, No. 2, 2013, 24201, https://doi.org/10.1103/PhysRevB.87.024201.

[7] G. Gutierrez, B. Johansson, Molecular Dynamics Study of Structural Properties of Glass Al_2O_3, Physical Review B, Vol. 65 , No. 10, 2002, 104202, https://doi.org/10.1103/PhysRevB.65.104202.

[8] V. V. Hoang, S. K. Oh, Simulation of Structural Properties and Structural Transformation of Glass Al_2O_3, Physica B: Condensed Matter, Vol. 352, 2004, pp. 73-85, https://doi.org/10.1016/j.physb.2004.06.057.

[9] L. T. Chinh, T. T. Nguyen, T. T. Nguyen, V. V. Le, Molecular Dynamics Simulation of Phase Transformation and Mechanical Behavior in Al_2O_3 Model, Vacuum, Vol. 167, 2019, pp. 175-181, https://doi.org/10.1016/j.vacuum.2019.06.010.

[10] N. N. T. Ha, N. V. Hong, P. K. Hung, Network Structure and Dynamics Heterogeneities in Al_2O_3 System: Insight from Visualization and Analysis of Molecular Dynamics Data, Indian Journal of Physics, Vol. 93 , No. 8, 2019, pp. 971-978, https://doi.org/10.1007/s12648-018-01358-7.

[11] A. K. Verma, P. Modak, B. K. Bijaya, First-principles Simulations of Thermodynamical and Structural Properties of Liquid Al_2O_3 Under Pressure, Physical Review B, Vol. 84, No. 17, 2011, pp. 174116, https://doi.org/10.1103/PhysRevB.84.174116.

[12] S. Davis, G. Gutiérrez, Structural, Elastic, Vibrational and Electronic Properties of Glass Al_2O_3 from Ab Initio Calculations, Journal of Physics: Condensed Matter, Vol. 23, No. 49, 2011, pp. 495401, https://doi.org/10.1088/0953-8984/23/49/495401.

[13] L. T. Ha, P. H. Kien, Domain Structural Transition and Structural Heterogeneity in GeO_2 Glass Under Densification, ACS omega, Vol. 5, No. 45, 2020, pp. 29092-29101, https://doi.org/10.1021/acsomega.0c03722.

[14] P. H. Kien, P. M. An, G. T. T. Trang, P. K. Hung, the Structural Transition Under Compression and Correlation between Structural and Dynamical Heterogeneity for Liquid Al_2O_3, International Journal of Modern Physics B, Vol. 33, No. 31, 2019, pp. 1950380, https://doi.org/10.1142/S0217979219503806.